Journal of Crystal Growth 51 (1981) 131–139

DIFFUSION COEFFICIENT AND SOLUBILITY OF Ge AND GaAs IN Pb AND APPLICATION TO LPE GROWTH OF Ge ON GaAs †

Anthony A. IMMORLICA, Jr. and Burt W. LUDINGTON *
Rockwell International Electronics Research Center, Thousand Oaks, California 91360, USA

Received 30 January 1980; manuscript received in final form 20 March 1980

Knowledge of the diffusion coefficient and solubility of solute atoms in liquid melts is required in order to accurately predict the diffusion limited growth rate of crystals nucleated from the liquid phase. In this work, diffusion coefficients and solubilities are determined independent of the growth process by measuring the weight loss of a semiconductor wafer after being placed in contact with a melt. Data are reported for the systems Ge in Pb and GaAs in Pb, over the temperature ranges normally employed in liquid phase epitaxy. Solubility data for eutectic Pb-Sn melts are also reported. Addition of Al or Ga to a Pb-Ge melt is found to greatly lower the solubility of GaAs in the melt; this facilitates the growth of p^+n Ge–GaAs heterodiodes by substantially reducing the possibility of substrate meltback. Ge layers are grown on ⟨111B⟩ GaAs substrates by a step-cooling technique. Excellent agreement between observed growth rates and those predicted from the diffusion coefficient and solubility data is obtained.

1. Introduction

Growth of single crystals from dilute metallic solutions by liquid phase epitaxy (LPE) is widely used for preparation of thin semiconductor layers. Typical growth apparatus employs a horizontal boat with a movable compartment that brings a saturated melt into contact with a seed crystal. Alternatively, vertical systems, in which a seed is dipped into a melt, have been used. Epxitaxial growth is normally driven by lowering the furnace temperature after melt–seed contact (equilibrium cooling) [1], having the seed somewhat cooler than the melt at the initial contact (step cooling) [1], employing a temperature gradient normal to the seed (constant temperature epitaxy) [2] or using a combination of these techniques. For most typical semiconductors grown by these methods, transport of solute atoms from the melt to the growing interface is usually governed primarily by a diffusion process. Growth rate is thus specified by a solution of the classical heat flow equation subject to the boundary conditions appropriate for the growth technique used. It is evident, then, that knowledge of the diffusion coefficient and solubility of the solute atoms in the liquid melt is a requisite for predicting crystal growth rates.

Diffusion coefficients for certain systems have been deduced by previous workers [3–7] who have taken the diffusion coefficient as' an adjustable parameter and have fitted the experimental data to an appropriate growth rate equation. While self-consistent results are reported, the technique does not necessarily lend itself to universal application, particularly since convection, consitutional supercooling and substrate dissolution can play a role to varying degrees in some epitaxial growth systems. The latter case is particularly true for heterojunction growths, since the growth melt is rarely near thermodynamic equilibrium with the seed crystal at the initiation of growth.

Measurement of solubility, or the liquids line of a phase diagram, is more straight forward. Typical methods include determination of the arrest of a cooling curve as the temperature of a melt of known constituents is lowered, or observation of the complete dissolution of a crust of solid solute on the surface of a melt as the temperatue is raised. In the latter method, solute density must be less than the melt

† Work supported by Air Force Office of Scientific Research under Contract No. F44620-76-C-0134.
* Present address: Energy Center, University of Pennsylvania, 3221 Walnut Street, Philadelphia, Pennsylvania, USA.

density at the liquidus temperature.

In this work, the diffusion coefficients and solubilities of solute atoms in liquid metals are determined by measuring the weight loss of a semiconductor wafer after it has been placed in contact with the melt. For diffusion coefficient determination, the contact time is kept short so that the melt appears "semi infinite;" the diffusion coefficient is then readily calculated by assuming an error function distribution of solute atoms in the melt. For solubility measurements, melt–seed contact is maintained long enough for the system to reach equilibrium. These procedures have been applied to the systems Ge and GaAs in Pb and eutectic PbSn. The effect of addition of p-type Ge dopants on solubilities in the Pb based system have also been studied. Excellent agreement between predicted and observed growth rates for Ge on GaAs is obtained, and application to growth of Ge–GaAs p^+n heterodiodes is described.

2. Experimental procedure

A standard liquid phase epitaxial growth system was employed in this study. The system consists of a horizontal graphite boat with a substrate recess and a 1.2 cm high sliding graphite melt compartment; both have identical cross-sectional areas of 2.4 cm^2. Metals of "six-nines" or better purity were employed; the Pb was etched in a mixture of acetic acid and hydrogen peroxide prior to loading into the system while the Sn was etched in a mixture of nitric acid, hydrofluoric acid and water. The Ge wafers were chemically–mechanically polished with Br–methanol, degreased, and then etched in CP4 just prior to the experiment. The GaAs wafers were degreased, etched in warm Caro's solution ($H_2SO_4 : H_2O_2 : H_2O = 3 : 1 : 1$), and then soaked in warm HCl.

Prior to loading, the crystal wafers were weighed on an electronic balance with 10 ug sensitivity. The LPE system was evacuated and then purged with Pd-purified H_2. For experiments involving GaAs, the furnace temperature was raised past 700°C to ensure complete removal of residual surface oxides. The furnace was then stabilized at the desired temperature, by using a controller capable of maintaining better than ±1/4°C/h. A "transparent" furnace with semi-transparent gold-coated pyrex walls allowed the operator to observe the melt surface during the experiment.

The diffusion coefficient of the solute atoms comprising the semiconductor wafer, in the liquid metal melt, was determined by bringing the two into momentary contact. As the wafer was dissolved by the solvent, a concentration gradient of solute atoms was established in the melt. The resulting concentration profile, $C(x, t)$, is given by a solution of the classic diffusion problem for a constant source:

$$C(x, t) = C_0 \operatorname{erfc}[x/2(Dt)^{1/2}] , \tag{1}$$

where C_0 is the solute molar solubility per unit volume of melt, D is the diffusion coefficient, x is distance into the melt and t is time.

Integration of eq. (1) from $x = 0$ to ∞ yields the total amount of dissolved solute:

$$Q = 2A \frac{\rho_m}{M_m} X_s \left(\frac{Dt}{\pi}\right)^{1/2} , \tag{2}$$

where Q is the number of moles of material dissolved, A is the wafer area, X_s is the equilibrium solubility expressed as atomic fraction, and ρ_m/M_m is the ratio of the melt density to gram molecular weight, i.e., the molar melt volume.

Expressing Q in terms of the weight loss, ΔW, in the time interval t, and solving for D, gives

$$D = \frac{\pi}{t} \left(\frac{1}{2AX_s} \frac{\Delta W}{\rho_m} \frac{M_s}{M_m}\right)^2 , \tag{3}$$

where M_s is the gram molecular weight of the solute. All terms on the right hand side of eq. (3) are known or can be measured.

In order to ensure the validity of the semi-inifinite melt approximation, the contact time t is chosen such that $Dt \ll L^2$, where L is the physical height of the melt. Typically, a contact time of 30 s was chosen so that the validity of the semi-infinite approximation was insured while yielding a wafer weight loss of several milligrams, which is easily measured.

By invoking eq. (1), the effect of the moving dissolution interface and the role of dissolution kinetics are ignored. Assumption of a stationary interface is quite reasonable, however, since the dissolved layer thickness (~1–2 μm) is several orders of magnitude less than the typical diffusion lengths (~500 μm) encountered in the measurement. The stationary interface assumption is, in fact, valid for most situa-

tions involving diffusion limited LPE growth [8]. Likewise, reaction kinetics are not judged to play a significant role in these measurements nor have they been shown to be a factor in most reported LPE growths in which thickness–time dependences of $t^{1/2}$ or $t^{3/2}$ are reported [1,3], depending on the growth technique. Growths dominated by interface kinetics would be expected to exhibit a t^2 dependence [9]. Furthermore, diffusion coefficients measured by the method reported here have given equivalent results when (100) and (111) oriented substrates were utilized.

For determination of solubility, the melt compartment was moved over the wafer and held long enough to ensure that the solvent was saturated with the solute material. Typically, this was on the order of 60 min. By observing the melt surface through the transparent furnace during this period, the operator could insure that the measurement was not influenced by precipitation. After saturation, the melt compartment was moved off the remaining source material and the weight lost by the wafer was determined after removal from the furnace. Generally, the melt wiped cleanly off the wafer; wafers were examined for residual melt droplets which were cleaned by warm HCl if necessary. The solubility is then given by the following:

$$X_s = \frac{\Delta W}{\Delta W + W_m M_s / M_m} , \tag{4}$$

where W_m is the initial weight of the pure melt.

3. Results and discussion

3.1. Diffusion coefficients

Diffusion coefficients for the Ge–Pb and GaAs–Pb systems were determined at three different temperatures; results are shown in fig. 1. Diffusion data can be approximated by an exponential relationship

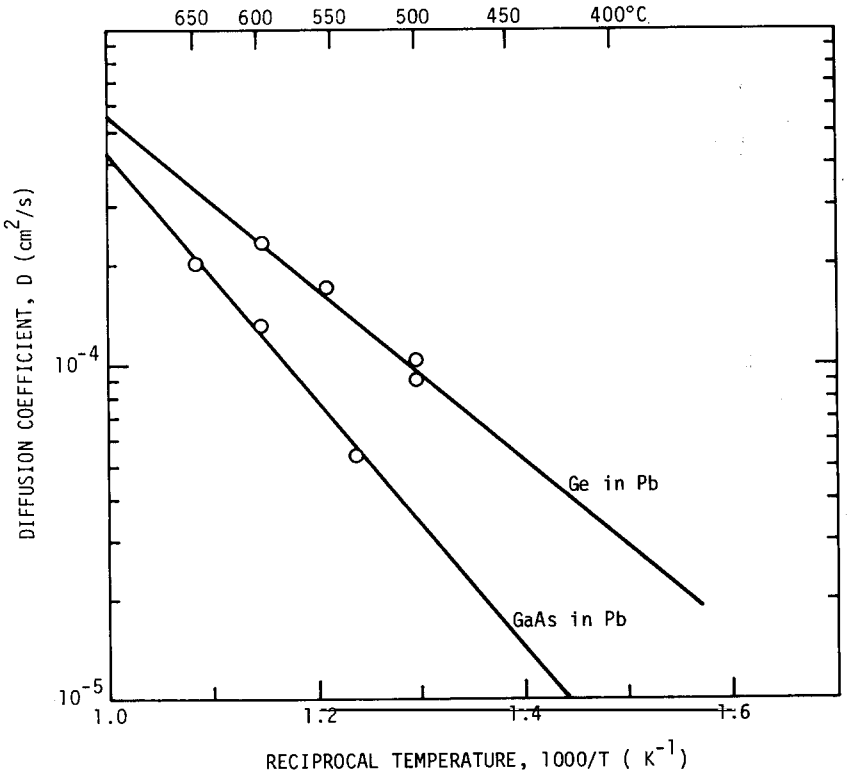

Fig. 1. Diffusion coefficient of Ge and GaAs in liquid Pb as a function of reciprocal temperature.

of the form

$$D = D_0 \exp(-E_a/kT), \quad (5)$$

where D_0 is a constant, E_a is an activation energy, T is the Kelvin temperature, and k is the Boltzmann constant. Values of D_0 and E_a are summarized in table 1.

Three assumptions are implicit in the diffusion coefficient measurement technique: (1) the melt is isothermal, (2) the melt appears semi-infinite, (3) the melt is stagnant. The first assumption, that of an isothermal melt, is clearly justified, as the thermal diffusivity in liquid metals is typically on the order of 0.1 to 0.5 cm^2/s, several orders of magnitude higher than the measured diffusion coefficients. If the melt is presumed to be stagnant, the second assumption is also justified since contact times, which were typically on the order of 30 s, resulted in a diffusion length of 500 μm, whereas L is approximately 1.2 cm. Assumption of a stagnant melt is not necessarily valid, however, as factors exist that may lead to convection, including thermal gradients, buoyancy effects (i.e., solute gradients) and mechanical stirring of the melt. However, while no attempt has been made in this study to quantify these effects, assumption of minimal convection appears reasonable in light of experimental growth results reported below which are in excellent agreement with predicted growth rates based on the diffusion coefficient measurement. This is true for all growth data that span growth times of 15 to 300 s, or factors of 1/2 to 10 times the diffusion coefficient measurement time. Thus, even though a constant weak convection may be present, the method yields self-consistent results, which give an "effective" diffusion coefficient, and is valuable for predicting growth rates in a given system.

Table 1
Diffusion constant and activation energy for Ge and GaAs in Pb

	D_0 (cm^2/s)	E_a (eV)
Ge in Pb	0.37	0.55
GaAs in Pb	3.18	0.76

3.2. Solubility

Solubility data were taken at several discrete temperatures over a 400–700°C temperature range and were fit to the exponential relationship for dilute solutions given by:

$$X_s = X_0 \exp(-\Delta H/nRT), \quad (6)$$

where ΔH is the enthalpy of the system, T is the temperature in degrees Kelvin, R is the universal gas constant and X_0 is a constant. The parameter n represents the number of moles of solute in the solution. Thus n equals 1 for Ge, but can vary from 1 to 2 for GaAs depending on the molecular species present.

Results are presented in fig. 2 for Ge and GaAs in

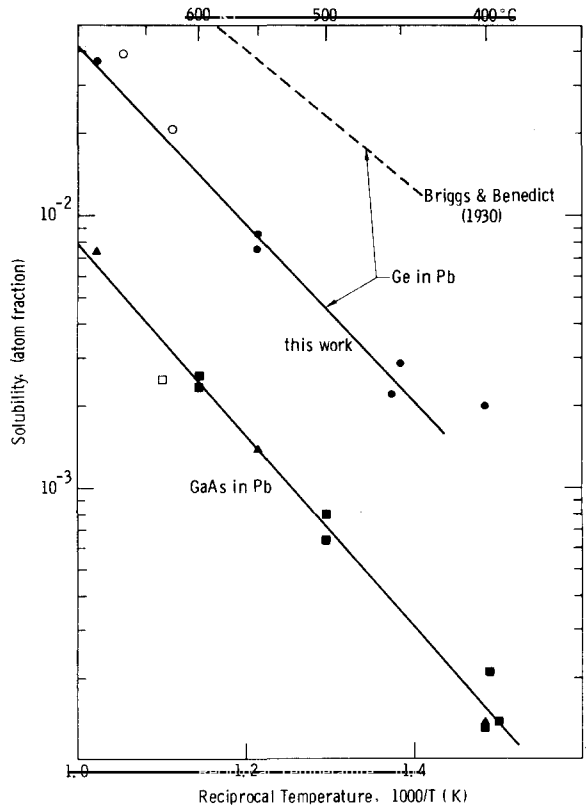

Fig. 2. Solubility versus reciprocal temperature. Dashed line is extrapolated from high temperature data of Briggs and Benedict [10] for Ge in Pb. Solid lines are best fits to our experimental data for Ge in Pb (•) and GaAs in Pb (■). The open circles and square are taken from refs. [11] and [12]. The triangles (▲) represent the solubility of GaAs in a saturated Pb–Ge melt.

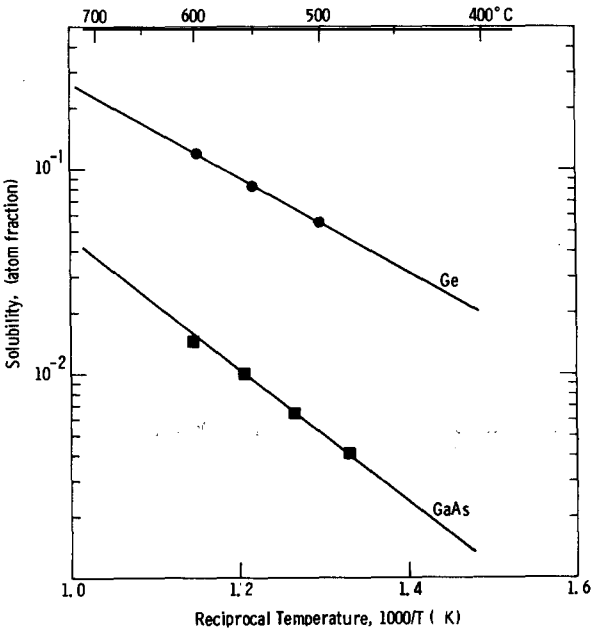

Fig. 3. Solubility versus reciprocal temperature of Ge (•) and GaAs (▪) in a eutectic solution of Pb and Sn.

Pb. Measurements were also taken for eutectic Pb–Sn solutions; these are given in fig. 3. The solid lines in the figures represent a best fit of eq. (6) to the data points represented by the solid squares and circles in the figures. The parameters of eq. (6) are given in table 2.

Also shown in fig. 2 are published data extrapolated from high temperature measurements by Briggs and Benedict [10] for Ge in Pb. Their discrepancy with the present work is not surprising in that they report considerable uncertainty in the arrest of a cooling curve for low concentrations of Ge in the melt. In an unpublished work by F.X. Hassion cited by Thurmond and Kowalchick [11], a solubility of 0.021 and 0.040 atomic fraction at 901 and 953 K,

Table 2
Solubility constant and enthalpy for Ge and GaAs in Pb and Pb–Sn

	X_0	$\Delta H/h$ (kcal/mole)
Ge in Pb	77.3	15.7
GaAs in Pb	32.4	16.5
Ge in Pb–Sn	58.3	10.7
GaAs in Pb–Sn	62.8	14.3

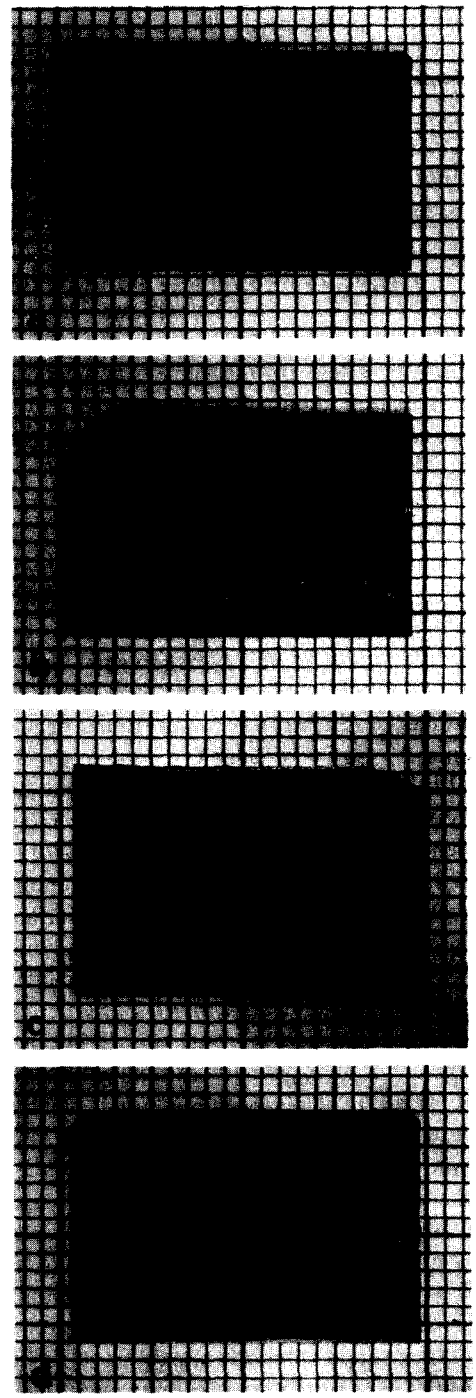

Fig. 4. Surface of GaAs substrate after equilibrating for 1 h at 550°C with a Pb melt containing various quantities of Al. Note decrease in solubility of GaAs with increasing amounts of Al: (a) 10×10^{-4}, (b) 5×10^{-4}, (c) 2.5×10^{-4}, (d) 1×10^{-4} atomic fraction Al in Pb.

respectively, is reported; this is also shown in the figure (open circles). These data are in much better agreement with the present work which extends knowledge of the Pb–Ge liquidus line down to 400°C. Similarly, our measurement of Pb–GaAs liquidus data also extends below the last reported results at 640°C by Green and Davies [12] (open square in fig. 2).

The triangular data points in fig. 2 represent the liquidus line of GaAs in a Pb solution saturated with Ge. It can be seen that the presence of Ge in the solution has no effect on the GaAs solubility over the range measured. Solubility measurements were also attempted for GaAs in Pb which had small amounts of Al. Aluminum is an attractive p-type dopant for Ge. Addition of Al to a Pb melt has a remarkable effect on the solubility of GaAs. While the Ge solubility over a 400 to 700°C temperature interval remained uneffected by the addition of 0.01 atomic fraction of Al, no GaAs solubility could be detected within the limits of the measurement; this implies that the solubility decreased at least two orders of magnitude. A similar result was found when small amounts of Ga were added to the melt. Further solubility measurements at 550°C as a function of Al concentration resulted in no observable interaction between a Ge saturated Pb melt and a GaAs substrate for Al atomic fractions of 10^{-3}. This is demonstrated in fig. 4, which is a photograph of the surface morphology of four GaAs substrates after equilibrating for 1 h at 550°C with Ge saturated Pb melts which contained various amounts of Al. For Al content of 5×10^{-4} atomic fraction, some surface interaction is observed and an apparent solubility of 4×10^{-4} atomic fraction of GaAs is calculated, which represents a factor of 4 suppression in the GaAs solubility. However, the surface morphology of these layers is not characteristic of simple meltback. The measured wafer weight loss may have been due to a combination of meltback and a solid–solid reaction between the Al and GaAs, which resulted in a compound that was etched by HCl in the post-cleaning procedures. Thus, the apparent solubility should be regarded as an upper limit. The significance of these measurements is in being able to grow a highly doped p-type layer of Ge on GaAs with no autodoping in the Ge layer or meltback of the GaAs layer at the initiation of growth.

4. Epitaxial growth and applications

In order to assess the validity of the results, Ge epitaxial layer thickness data were examined. The Ge layers were grown on ⟨111B⟩ GaAs substrates from supercooled Pb melts by using the step cooling growth technique [1]. For this method of growth, the layer thickness, d, as a function of time, t, is given by

$$d = (2\Delta T_s/C_s m)(Dt/\pi)^{1/2} , \quad (7)$$

where ΔT_s represents the supercooling in degrees, C_s is the concentration of Ge in the solid, and m is the inverse slope of the liquidus line. Data are presented in fig. 5 for layers grown at 575°C with a 4°C supercooled melt. The layer thicknesses were determined by angle lap techniques. The solid line in the figure is the theoretically calculated thickness from eq. (7); the diffusion coefficient of 2×10^{-4} cm^2/s determined in this work was used in this calculation. Excellent agreement is seen between the growth data and that predicted from eq. (7) where the solubility and diffusion coefficient data determined in this study are used.

Layers were also grown at temperatures as low as 400°C using melts supercooled to 14°C. Larger values of supercooling are necessary at the lower growth temperatures to avoid gross meltback. In spite of the relatively large amount of supercooling employed, excellent surface morphology is obtained on the ⟨111B⟩ orientation as shown in fig. 6. On the ⟨100⟩ orientation, however, pyramidal Ge growth hillocks,

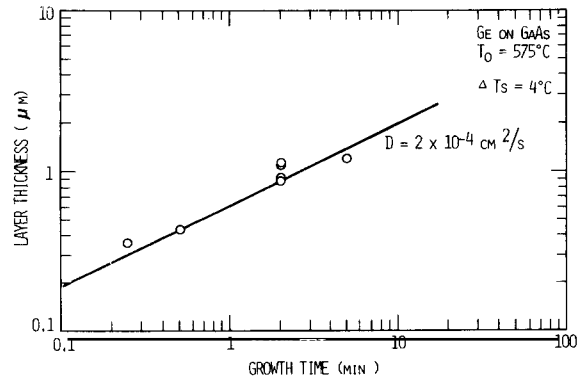

Fig. 5. Thickness data of Ge epitaxial layers as a function of growth time. The solid line is the theoretical thickness based on eq. (7).

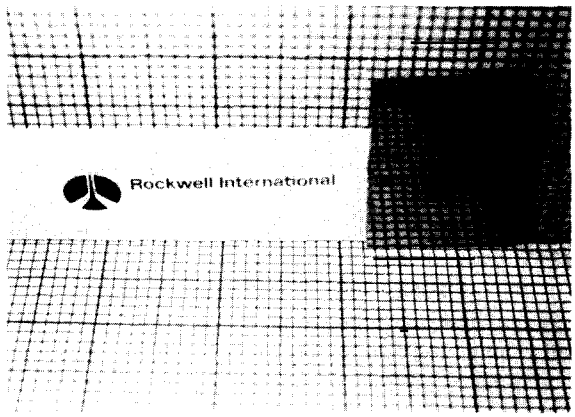

Fig. 6. Photograph showing mirror-like morphology of Ge layer grown on ⟨111B⟩GaAs.

as shown in fig. 7, were frequently observed when layers were grown from melts supercooled sufficiently to avoid meltback.

Step cooling was found to be the most effective technique for eliminating macroscopic meltback when using undoped melts. Sharp metallurgical interfaces are routinely obtained, as shown in fig. 8a, whereas a high tendency for gross meltback occurred in growths employing equilibrium cooling as shown in fig. 8b. Such later results suggest that strong localized density gradients can be formed due to the competing processes of dissolution and growth. It is clear then, that some critical amount of melt supersaturation is required to provide an effective driving force to favor growth over macroscopic dissolution during the initial melt–seed contact. However, as the melt and seed are never in thermodynamic equilibrium for heterojunction systems, microscopic dissolution of a few atomic layers cannot be completely ruled out even though planar interfaces are obtained. This may explain the

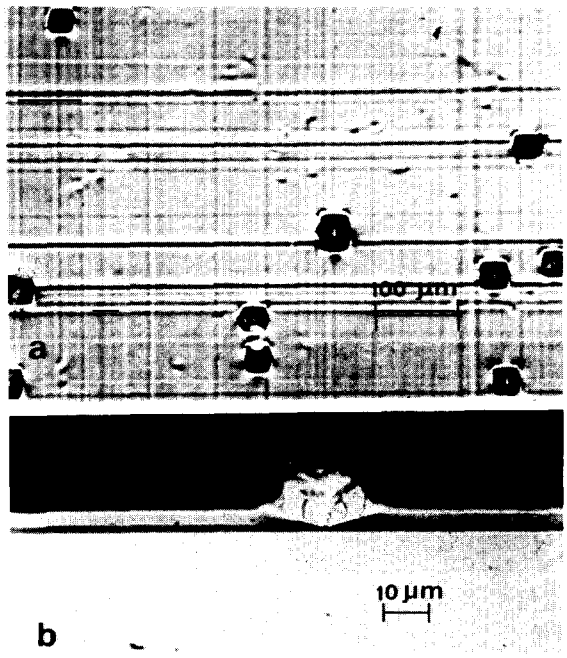

Fig. 7. (a) Photograph of a Ge layer showing hillocks observed for growths on ⟨100⟩GaAs. (b) Cleaved section of the above layer.

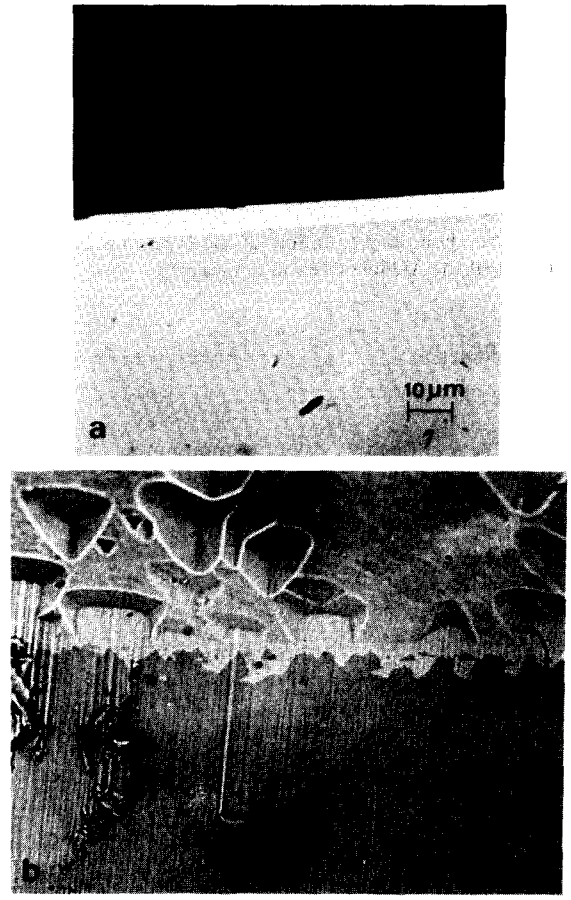

Fig. 8. (a) Cleaved Ge–GaAs structure; the Ge was grown by step cooling. (b) Angle lapped section of a Ge–GaAs structure exhibiting meltback of the GaAs substrate; the Ge was grown by equilibrium cooling.

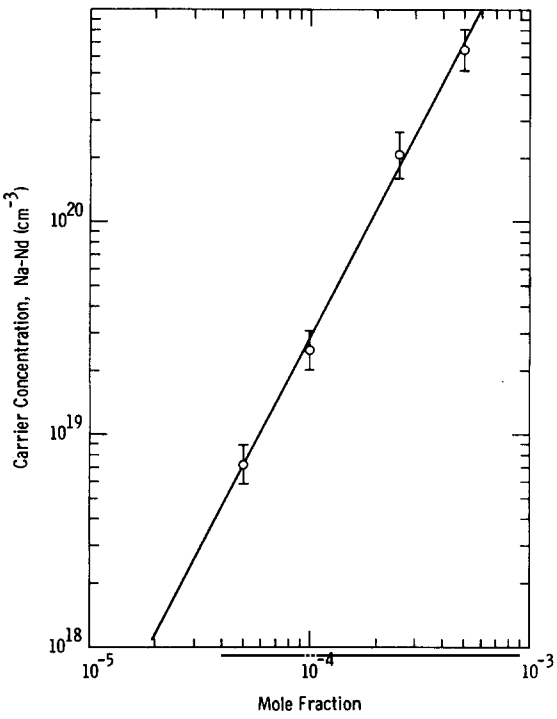

Fig. 9. Net hole concentration of Ge layers on GaAs as a function of the Al mole fraction in the melt.

relatively high carrier densities ($>10^{17}$ cm^{-3}) observed in layers grown from undoped melts. By doping the melt with Al or Ga, however, the solubility of GaAs in the melt is greatly suppressed as shown above, and no dissolution would be expected.

Using ternary Pb–Ge–Al melts with a range of Al atomic fractions varying between 5×10^{-5} and 5×10^{-4}, a series of Ge layers were grown on ⟨111B⟩GaAs at 575°C. All layers exhibited the excellent mirror-like surface morphology shown in fig. 6. The net hole concentration, determined by Van der Pauw measurements, is shown in fig. 9 as a function of the mole fraction of Al in the melt, X_{Al}. Meltback suppression has also been obtained with Ga doped melts and hole carrier concentrations as high as 3×10^{20} cm^{-3} have been achieved. An application of this meltback suppression technique might be in the growth of emitter layers for Ge–GaAs heterojunction bipolar transistors or for p^+ contacts to microwave diodes, applications in which it is critical that the underlying GaAs layer not be disturbed.

Meltback suppression has been exploited in the formation of rectifying p^+ Ge contacts to n-type GaAs in lieu of the commonly used Schottky barrier or GaAs p^+n homojunctions. The single crystal Ge

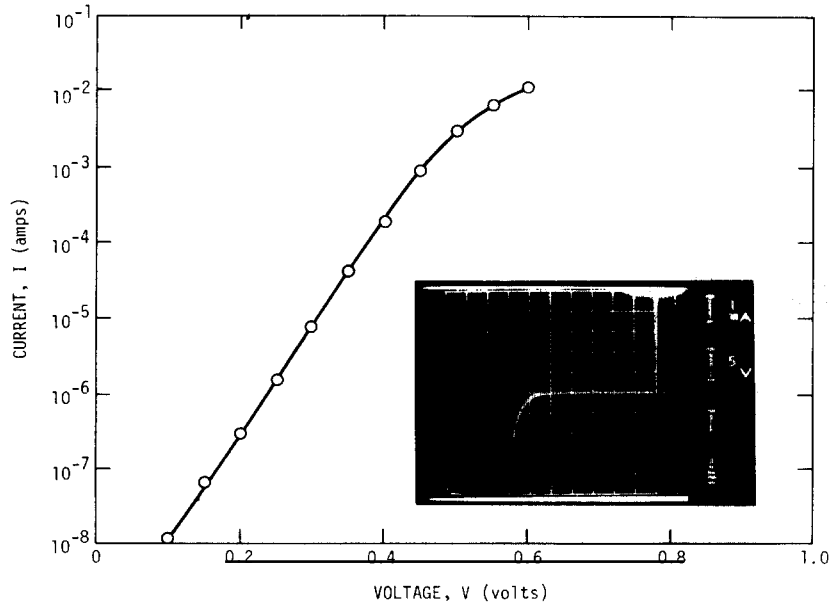

Fig. 10. Log-linear plot of the forward current–voltage characteristics of a Ge–GaAs heterojunction. The insert shows the reverse characteristics.

contact, which has an excellent lattice match to GaAs, could be expected to exhibit a higher reliability than metal–GaAs contacts while yielding a lower ohmic resistance and higher thermal conductivity than p-type GaAs. Typical current voltage characteristics of an LPE grown p^+ Ge–GaAs heterojunction are shown in fig. 10. The forward characteristics follow a thermionic emission–diffusion model with an ideality factor of 1.19 and the reverse breakdown voltage of 30 V approximates the expected value for the 4×10^{16} cm^{-3} n-type GaAs layer. The GaAs was grown in situ at 700°C using a covered melt compartment while the Ga doped Ge layer was grown at 430°C after rapidly cooling and stabilizing the furnace at the Ge growth temperature. No evidence of meltback was detected on a cleaved surface and the capacitance–voltage characteristics of these devices exhibit a square law response with a $1/C^2$ versus V plot yielding a voltage intercept of 1.0 V.

5. Summary

A technique has been described for determining the diffusion coefficient and solubility of solute atoms in liquid metals by using a dissolution process. The systems Pb–Ge, Pb–GaAs, PbSn–Ge, and PbSn–GaAs have been studied and results are reported. This technique is particularly applicable to situations involving LPE growth and yields data that accurately predict growth rates in the systems reported in this work.

During the course of this work, it was found that addition of small amounts of Al or Ga to a Pb–Ge melt greatly suppresses the GaAs solubility in the melt. This facilitates the growth of p^+n Ge–GaAs heterojunctions as it eliminates the possibility of substrate meltback. Growth of p^+n Ge–GaAs heterodiodes has been demonstrated using this meltback suppression technique. Presumably, other elements can be found which suppress GaAs solubility and are electrical neutral in Ge, facilitating the growth of undoped Ge layers on GaAs.

References

[1] J.J. Hsieh, J. Crystal Growth 27 (1974) 49.
[2] S.I. Long, J.M. Ballantyne and L.F. Eastman, J. Crystal Growth 26 (1974) 13.
[3] D.L. Rode, J. Crystal Growth 20 (1973) 13.
[4] L.R. Dawson, J. Crystal Growth 27 (1974) 86.
[5] R.L. Moon and S.I. Long, J. Crystal Growth 32 (1976) 68.
[6] R.L. Moon and J. Kinoshita, J. Crystal Growth 21 (1974) 149.
[7] I. Crossley and M.B. Small, J. Crystal Growth 11 (1971) 157.
[8] M.B. Small and J.F. Barnes, J. Crystal Growth 5 (1969) 9.
[9] E.A. Giess and R. Chez, in: Epitaxial Growth, Ed. J.W. Matthews (Academic Press, 1975) p. 206.
[10] T.R. Briggs and W.S. Benedict, J. Phys. Chem. 34 (1930) 173.
[11] C.D. Thurmond and M. Kowalchik, Bell Syst. Tech. Journal 39 (1960) 169.
[12] P.D. Green and I.C.A. Davies, J. Less Common Metals 34 (1974) 267.